Investigation of anisotropic velocity distribution functions using numerical solutions of the stationary Vlasov equation

Gabriel Voitcu[1], Costel Bunescu[1], Marius M. Echim[1,2]

[1]*Institute for Space Sciences, Magurele, Romania*

[2]*Belgian Institute for Space Aeronomy, Bruxelles, Belgium*

Contact: gabi@venus.nipne.ro

1 Abstract

In this paper we investigate the anisotropy of velocity distribution functions (VDF) of a collisionless plasma convecting in non-uniform distributions of the electromagnetic field. The VDF is reconstructed in various spatial regions by integrating numerically the characteristics of the stationary Vlasov equation. The method is applied to simulate the interaction between an electron and a proton cloud and a non-uniform, sheared distribution of the magnetic field with a superimposed electric field. We consider a non-uniform distribution of the electric field that conserves the zero order drift. The fields are steady-state and one-dimensional (depend on x only). The variation is concentrated in a limited region, like in kinetic tangential discontinuities. Test-particles (protons and electrons) are injected from sources aligned along the x-axis with initial velocities distributed according to a displaced Maxwellian with an average velocity $V_{0x}\neq 0$; their trajectories are integrated numerically. We use the Liouville theorem to "propagate" an initial VDF along the numerically integrated trajectories and to reconstruct it at the right side of the transition region. We consider a narrow transition, where the magnetic field varies rapidly over distances of the order of the Larmor radius, as well as an adiabatic variation of **B**. The numerical results illustrate the contribution of the charge-dependent gradient-B drift on shaping the overall dynamics of the ensemble of particles as well as on imprinting anisotropies of the VDF inside the propagating beam. Our numerical solutions suggest that the velocity filtering due to the grad-B drift may perhaps contribute to the formation of nongyrotropic velocity distribution functions observed in space plasma. The solutions are compared with simulations and experimental data obtained in the tail of the Earth's magnetosphere.

2 Numerical Modeling

The evolution of $f_\alpha(\boldsymbol{r},\boldsymbol{v},t)$, the velocity distribution function (VDF) of each component species α, is described, in the absence of binary collisions, by the Vlasov equation:

$$\frac{\partial f_\alpha}{\partial t}+\boldsymbol{v}\cdot\frac{\partial f_\alpha}{\partial \boldsymbol{r}}+\frac{q_\alpha}{m_\alpha}(\boldsymbol{E}+\boldsymbol{v}\times\boldsymbol{B})\cdot\frac{\partial f_\alpha}{\partial \boldsymbol{v}}=0$$

In the stationary case ($\partial/\partial t=0$) the characteristics of the Vlasov equation coincide with the trajectories of the particle with mass m_α and charge q_α moving in the electromagnetic field given by $\boldsymbol{E}(\boldsymbol{r})$ and $\boldsymbol{B}(\boldsymbol{r})$. Thus the characteristics of the Vlasov equation can be obtained by solving the equation of motion:

$$\frac{d^2\boldsymbol{r}}{dt^2}=\frac{q_\alpha}{m_\alpha}\left(\boldsymbol{E}+\frac{d\boldsymbol{r}}{dt}\times\boldsymbol{B}\right)$$

It must be mentioned that the magnetic and electric fields used to integrate equation of motion are due to external distributions only, the self-consistent contribution of plasma being neglected.

The magnetic field is typical for a one-dimensional tangential discontinuity (TD) as described by kinetic models. The magnetic field is stationary, depends only on x-coordinate and its tangential component varies between two asymptotically states as described by:

$$\boldsymbol{B}(x)=\frac{\boldsymbol{B}_1}{2}erfc\left(\frac{x}{L}\right)+\frac{\boldsymbol{B}_2}{2}\left[2-erfc\left(\frac{x}{L}\right)\right]$$

where L represents the characteristic scale length of the discontinuity; $\boldsymbol{B}_1$ and $\boldsymbol{B}_2$ denotes the values of $\boldsymbol{B}$ at $x=-\infty$ ("left hand side"), respectively at $x=+\infty$ ("right hand side"); *erfc* is the complementary error function.

The electric field is non-uniform and is everywhere normal to the magnetic induction $\boldsymbol{B}$. The parallel component of the electric filed is everywhere equal to zero. The electric field intensity is computed such that the zero order (or electric) drift, $\boldsymbol{U}_E$, is conserved:

$$\boldsymbol{E}(x)=\boldsymbol{B}(x)\times\boldsymbol{U}_E$$

The initial velocity distribution function of species α, injected at the "left hand side" of the TD, is described by a displaced Maxwellian with a bulk velocity, $\boldsymbol{V}_0$, parallel to the positive x-axis and perpendicular both to the discontinuity surface and the asymptotic field $\boldsymbol{B}_1$:

$$f_\alpha(v_x,v_y,v_z)=N_0\left(\frac{m_\alpha}{2\pi kT_0}\right)^{3/2}e^{-\frac{m_\alpha\left[(v_x-V_0)^2+v_y^2+v_z^2\right]}{2kT_0}}$$

N_0 and T_0 are the initial density and temperature of species α. The particles are injected from N sources aligned along x-axis; n particles from each source. The phase space is fairly well sampled when the total number of injected particles is of the order of 10^6.

The VDF is reconstructed at different moments of time by applying the Liouville theorem: $df/dt=0$ along each particle's orbit.

The numerical method of integration is based on a Cash-Karp Runge-Kutta fifth order algorithm with adaptive step size. The numerical codes have been developed on a Linux cluster running MPI.

3 Results

Table 1 - The values of the simulation parameters

N_0 (m^{-3})	T_0 (keV)	V_0 (km/s)	B_{1z} (nT)	L (km)	N	n	x_0 (km)	Δx_0 (km)	Δt (s)
10^4	7	200	-30, -60, -90	6800	6	$3\cdot10^5$	-8110	100	150

⇒ N_0 is the initial density of protons;
⇒ T_0 is the initial temperature of protons;
⇒ V_0 is the initial bulk velocity of protons;
⇒ B_{1z} is the asymptotic magnetic induction at the "left hand side" of TD;
⇒ L is the characteristic scale length of the TD;
⇒ N is the number of sources aligned along x-axis;
⇒ n is the number of protons injected from each source;
⇒ x_0 is the position of the first source;
⇒ Δx_0 is the distance between two adjacent sources;
⇒ Δt is the time interval of the simulation;

In this paper we discuss results obtained for an adiabatic discontinuity, $L>>R_{Li}$, with R_{Li} the proton Larmor radius. We investigate three asymptotic values of the magnetic field equal to 30 nT, 60 nT and 90 nT.

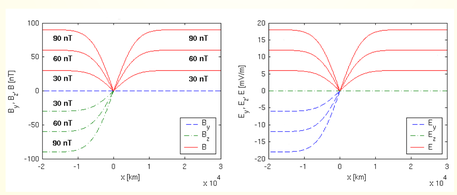

Figure 1 - The magnetic field distribution (left panel) and the electric field distribution (right panel) in the simulation domain. In x=0 the magnetic and electric field intensity is equal to zero.

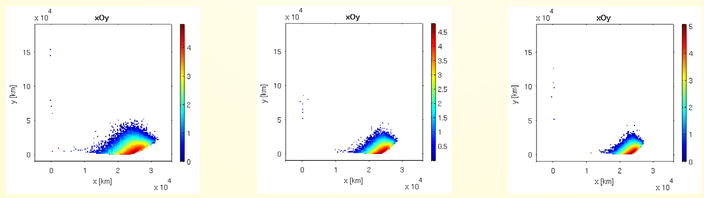

Figure 2 - The position of protons in the xOy plane, at the end of the simulation. The local number density is color coded. The asymptotic magnetic field is equal to 30 nT (left panel), 60 nT (middle panel) and 90 nT (right panel). The number density is computed on a mesh with 120x120 bins.

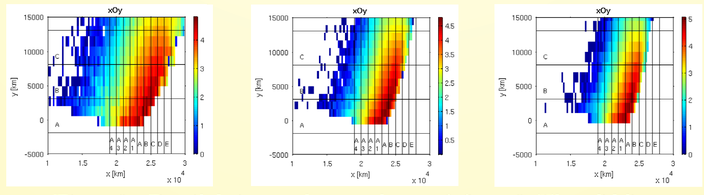

Figure 3 - Detailed view on the central area of figure 2. The solid lines illustrate the bins for which the VDF of protons is reconstructed with the method based on the Liouville theorem. The panels correspond to various asymptotic magnetic fields: 30 nT (left), 60 nT (middle) and 90 nT (right).

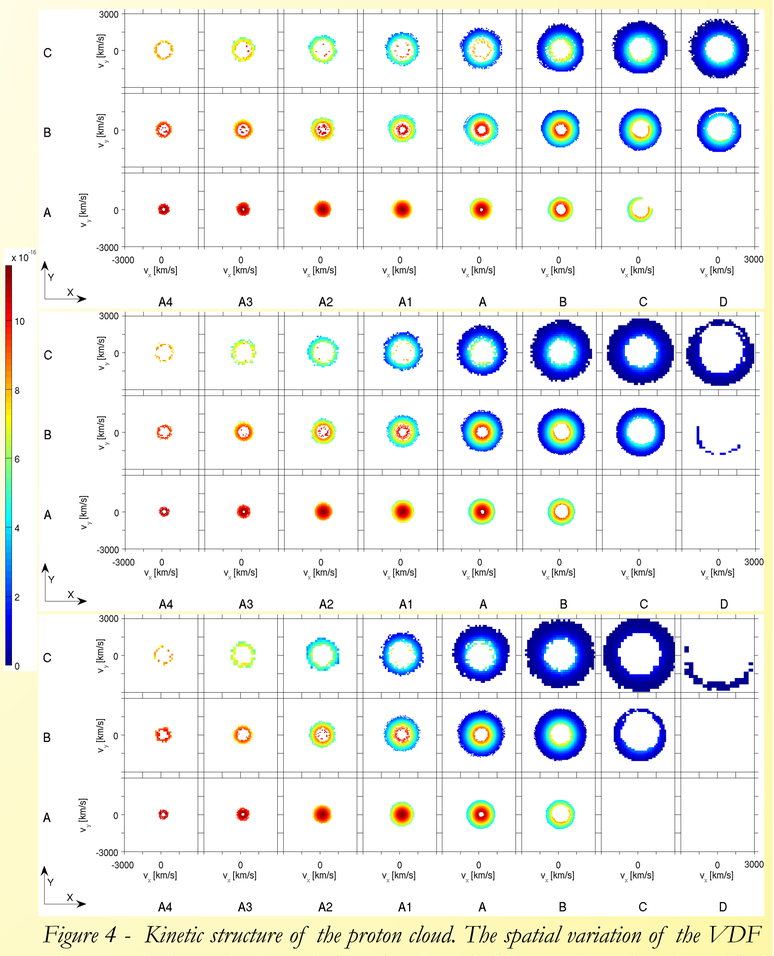

Figure 4 - Kinetic structure of the proton cloud. The spatial variation of the VDF of protons is shown for the mesh defined in figure 3. Note the formation of a void of particles in the central region of the VDF (row C in all panels). Non-gyrotropic distributions are observed at the frontside of the cloud. The three panels correspond to three asymptotic magnetic fields: 30 nT (top), 60 nT(middle) and 90 nT (bottom).

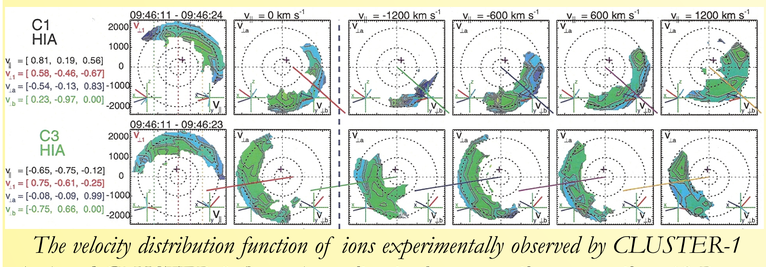

The velocity distribution function of ions experimentally observed by CLUSTER-1 (top) and CLUSTER-3 (bottom) sattelites in the terrestrail magnetotail, at 18 R_E, on 1 October 2001 (Wilber et al., 2004).

4 Discussion & Conclusions

Figure 2 shows that the proton cloud penetrates the TD and moves as such into the "right hand side" region. The dynamics of the proton cloud reveals asymmetries for all three values of the asymptotic magnetic field. The protons are scattered in the positive direction of the y-axis. The asymmetric expansion of the cloud is due to the positive gradient-B drift, acting in the discontinuity region. From figure 2 it can be seen that the spatial scattering of the protons varies inverse proportionally with the asymptotic value of the magnetic field. This confirms the role of the gradient-B drift that varies proportionally with $|\nabla B|/B^2$. On the other hand, the Larmor radius varies inverse proportionally with the magnetic induction such that the proton cloud dimensions in the xOy plane are smaller for a larger values of the asymptotic magnetic field intensity, as can be seen in figure 2. Figure 4 shows an interesting property of the VDF: the formation of a void region in the central part of the VDF. This effect is observed in spatial regions close to the lateral wings of the cloud. The area of the void formed in the space of perpendicular velocities varies with the distance from the center of the cloud. It is thus suggested that the edges of the cloud are mainly populated by the most energetic particles from the initial distribution. Since everywhere $\boldsymbol{E}$ is perpendicular to $\boldsymbol{B}$, there is no electrostatic acceleration. We conjecture that the physical mechanism that introduces this anisotropy of the VDF is related to the expansion of the cloud in the $+Oy$ direction. It is thus a finite Larmor effect due to the gradient-B drift. The anisotropy observed in the region of the propagation front is a non-local effect which we associate to the remote sensing of particles. Similar conjectures have been made by *Lee et al.* (2004) for in-situ magnetospheric data. These authors did not explain the formation of the void. VDFs with anisotropic features resembling the ones illustrated in this study have been observed experimentally in the terrestrial magnetosphere close to the neutral sheet.

5 References

[1] T. W. Speiser, J. Geophys. Res. 70, 4219 (1965).
[2] T. W. Speiser, J. Geophys. Res. 72, 3919 (1967).
[3] J. W. Eastwood, Planet. Space Sci. 20, 1555 (1972).
[4] J. W. Eastwood, Planet. Space Sci. 23, 1 (1975).
[5] K. D. Cole, Planet. Space Sci. 24, 515 (1976).
[6] K. D. Cole, Phys. Plasmas 3, 2717 (1996).
[7] P. L. Rothwell, M. B. Silevich, L. P. Block, C. G. Falthammar, J. Geophys. Res. 100, 14875 (1995).
[8] M. M. Echim, Cosmic Research 40, 534 (2002).
[9] T. W. Speiser, D. J. Williams, H. A. Garcia, J. Geophys. Res. 86, 723 (1981).
[10] L. R. Lyons, T. W. Speiser, J. Geophys. Res. 87, 2276 (1982).
[11] D. J. Williams, T. W. Speiser, J. Geophys. Res. 89, 8877 (1984).
[12] D. B. Curran, C. K. Goertz, T. A. Whelan, Geophys. Res. Lett. 14, 99 (1987).
[13] D. B. Curran, C. K. Goertz, J. Geophys. Res. 94 (1989).
[14] S. Chandrasekhar, Plasma Physics, University of Chicago Press (1960).
[15] J. L. Delcroix, A. Bers, Physique des plasmas, Savoirs Actuels-InterÉditions/CNRS Éditions, Paris (1994).
[16] A. Sestero, Phys. Fluids 7, 44 (1964).
[17] J. Lemaire, L. F. Burlaga, Astrophys. Space Sci. 45, 303 (1976).
[18] M. Roth, J. DeKeyser, M. M. Kuznetsova, Space Science Reviews 76, 251 (1996).
[19] G. Schmidt, Phys. Fluids 3, 961 (1960).
[20] M. Galvez, G. Gisler, C. Barnes, Phys. Fluids B 2(3), 516 (1990).
[21] D. S. Cai, O. Buneman, Phys. Fluids B 4(4), 1033 (1992).
[22] M. Wilber et al., Geophys. Res. Lett. 31, (2004).
[23] E. Lee et al., Geophys. Res. Lett. 31, (2004).